

Mechanistic and structural basis for inhibition of copper trafficking by platinum anticancer drugs

Alessia Lasorsa, Maria Incoronata Nardella, Antonio Rosato, VALENTINA MIRABELLI, Rosanna Caliandro, Rocco Caliandro, Giovanni Natile, and Fabio Arnesano

J. Am. Chem. Soc., **Just Accepted Manuscript** • DOI: 10.1021/jacs.9b05550 • Publication Date (Web): 08 Jul 2019

Downloaded from <http://pubs.acs.org> on July 8, 2019

Just Accepted

“Just Accepted” manuscripts have been peer-reviewed and accepted for publication. They are posted online prior to technical editing, formatting for publication and author proofing. The American Chemical Society provides “Just Accepted” as a service to the research community to expedite the dissemination of scientific material as soon as possible after acceptance. “Just Accepted” manuscripts appear in full in PDF format accompanied by an HTML abstract. “Just Accepted” manuscripts have been fully peer reviewed, but should not be considered the official version of record. They are citable by the Digital Object Identifier (DOI®). “Just Accepted” is an optional service offered to authors. Therefore, the “Just Accepted” Web site may not include all articles that will be published in the journal. After a manuscript is technically edited and formatted, it will be removed from the “Just Accepted” Web site and published as an ASAP article. Note that technical editing may introduce minor changes to the manuscript text and/or graphics which could affect content, and all legal disclaimers and ethical guidelines that apply to the journal pertain. ACS cannot be held responsible for errors or consequences arising from the use of information contained in these “Just Accepted” manuscripts.

Mechanistic and structural basis for inhibition of copper trafficking by platinum anticancer drugs

Alessia Lasorsa¹†, Maria I. Nardella¹†, Antonio Rosato¹, Valentina Mirabelli²,
Rosanna Caliandro^{3,4}, Rocco Caliandro², Giovanni Natile¹, Fabio Arnesano^{1*}

¹ Department of Chemistry, University of Bari “Aldo Moro”, via Orabona, 4, 70125 Bari, Italy

² Institute of Crystallography, CNR, via Amendola, 122/o, 70126 Bari, Italy

³ Bioorganic Chemistry and Bio-Crystallography laboratory (B(2)Cl), Faculty of Science and Technology, Free University of Bolzano, Piazza Università 5, 39100 Bolzano, Italy.

⁴ Institute of Crystallography, CNR, Area Science Park Basovizza, 34149 Trieste, Italy.

†These authors equally contributed to the work

* To whom correspondence should be addressed. E-mail: fabio.arnesano@uniba.it

Abstract

Copper (Cu) is required for maturation of cuproenzymes, cell proliferation, and angiogenesis and its transport entails highly specific protein-protein interactions. In humans, the Cu chaperone Atox1 mediates Cu(I) delivery to P-type ATPases Atp7a and Atp7b (the Menkes and Wilson disease proteins, respectively), which are responsible for Cu release to the secretory pathway and excess Cu efflux. Cu(I) handover is believed to occur through the formation of three-coordinate intermediates where the metal ion is simultaneously linked to Atox1 and to a soluble domain of Cu-ATPases, both sharing a CxxC dithiol motif. The ultra-high thermodynamic stability of chelating S-donor ligands secures the redox-active and potentially toxic Cu(I) ion, while their kinetic lability allows facile metal transfer. The same CxxC motifs can interact with and mediate the biological response to antitumor platinum drugs, which are among the most used chemotherapeutics. We show that cisplatin and an oxaliplatin analogue can specifically bind to the heterodimeric complex Atox1-Cu(I)-Mnk1 (Mnk1 is the first soluble domain of Atp7a), thus leading to a kinetically stable adduct that has been structurally characterized by solution NMR and X-ray crystallography. Of the two possible binding configurations of the Cu(I) ion in the cage made by the CxxC motifs of the two proteins, one (bidentate Atox1 and monodentate Mnk1) is less stable and more reactive toward *cis*-Pt(II) compounds, as shown by using mutated proteins. A Cu(I) ion can be retained at the Pt(II) coordination site, but can be released to glutathione (a physiological thiol) or to other complexing agents. The Pt(II)-supported heterodimeric complex does not form if Zn(II) is used in place of Cu(I) and transplatin instead of cisplatin. The results indicate that Pt(II) drugs can specifically affect Cu(I) homeostasis by interfering with the rapid exchange of Cu(I) between Atox1 and Cu-ATPases, with consequences on cancer cell viability and migration.

Introduction

Copper trafficking pathways require high protein-protein specificity, and generally involve a Cu chaperone that binds and delivers Cu to specific targets and organelles. In humans, Atox1 delivers Cu(I) to the metal-binding domains (MBDs) of Atp7a and Atp7b (the Menkes and Wilson disease proteins, respectively), two Cu(I)-transporting ATPases located in the Golgi¹; each ATPase has six soluble MBDs, which have been shown to interact differently with Atox1 in a Cu-dependent manner²⁻⁴. Both Atox1 and the MBDs bind one Cu(I) through two cysteine (Cys) residues located in a conserved CxxC motif⁵, and Cu(I) transfer is believed to occur via an Atox1-Cu(I)-MBD complex⁶. In cells exposed to high Cu levels, Cu(I) exchange between Atox1 and MBDs promotes Atp7a translocation from the trans-Golgi network (TGN) to the plasma membrane or cytosolic vesicles^{7,8}.

Enhanced Cu trafficking has been associated with various types of cancer, where Cu is required for angiogenesis, cell proliferation and metastasis^{9,10}. This has stimulated numerous approaches aiming at designing compounds able to interfere with Cu transport¹¹. A small molecule, selected among a library of compounds, was shown to target the Cu delivery pathway to the secretory compartment, by destabilizing the interface between the Cu(I) chaperone Atox1 and the acceptor domains of Cu(I)-ATPases, thus selectively reducing cancer cell proliferation and significantly attenuating tumor growth in mouse models¹².

Pt-based anticancer drugs used in the clinics, cisplatin, oxaliplatin and carboplatin (Fig. 1a), have the ability to target sulfur-containing metal-binding sites in Cu transporters¹³⁻¹⁷ and such behavior was shown to influence the cellular pharmacology of Pt drugs, either in terms of sensitivity or of resistance¹⁸⁻²⁰. Thus, Cu transporters have been proposed to be involved in Pt cellular uptake and subcellular distribution to different compartments and organelles.

Although nuclear DNA is the ultimate target of cisplatin, only a few percent (1-4%) of intracellular cisplatin forms adducts with nuclear DNA²¹⁻²⁶. The remaining part readily reacts with thiol-containing molecules inside the cytoplasm, including glutathione (GSH) and metallothioneins (MTs)^{27,28}.

As a matter of fact, cisplatin can exert prominent cytotoxicity also in enucleated cells (cytoplasts)²⁹⁻³¹. Therefore, the cytostatic/cytotoxic effects do not depend solely on the genotoxic activity of cisplatin, but can originate from both nuclear and cytoplasmic signaling pathways³²⁻³⁴.

The molecular mechanisms that underlie the cytotoxic potential of cytoplasmic drugs are still poorly understood, but may involve the accumulation of reactive oxygen species (ROS)^{30,33}.

1
2
3 It was found that cells treated with cisplatin for prolonged periods often develop acquired resistance
4 ^{35–37} and that such a resistance is in part associated to higher expression levels of Atox1 ^{38,39} and
5 Cu(I)-ATPases ^{40,41}. In particular, it has been reported that overexpression of Atp7a in human
6 carcinoma cells could result in the development of resistance ⁴², which is not necessarily associated
7 to enhanced efflux of cisplatin, but may be due to altered Pt intracellular distribution (overexpressed
8 transporters favoring drug accumulation in peripheral subcellular compartments) ^{40,43}.

9
10 We have shown that, following an ATP concentration jump, Atp7a or Atp7b embedded in
11 microsomes adsorbed on a gold electrode-supported membrane, can translocate Pt(II) cations, thus
12 inducing a current transient ⁴⁴. Moreover, Pt(II) drugs can inhibit the active transport of Cu(I) by the
13 ATPases and, viceversa, Cu(I) can inhibit the translocation of Pt(II) cations. However, we failed to
14 observe Pt transfer between Atox1 and the first soluble Cu(I)-binding domain of Menkes ATPase
15 under close to physiological conditions, i.e. in the presence of GSH as reducing agent ⁴⁵.

16
17 We and others observed that preloading with Cu(I) can foster the interaction with Pt drugs of the
18 dithiol motifs of Cu(I) transporters ^{44–47}, thus we deemed of crucial importance to characterize the
19 interaction of cisplatin and oxaliplatin with the Cu(I)-mediated complex of Atox1 and the first
20 soluble domain of Atp7a (Mnk1 hereafter).

21
22 The present work focuses on the reactivity of Cu(I) and Pt(II) (in the form of cisplatin and
23 oxaliplatin) with the proteins Atox1 and Mnk1. The formation of adducts has been studied by NMR
24 spectroscopy, HPLC/ESI-MS and UV-vis spectrophotometry. The results support the idea that
25 cisplatin can interfere with copper trafficking by forming stable mono- and hetero-dimeric adducts
26 with the proteins in the presence of Cu(I). Site-directed mutagenesis studies on Atox1 and Mnk1
27 were also performed to investigate the role of individual cysteines in the formation of adducts with
28 cisplatin, confirming that at least one Cys from each partner is necessary to form the heterodimeric
29 adduct. We also demonstrate that the Pt-bridged heterodimeric species does not form if transplatin
30 is used in place of cisplatin or Zn(II) is used in place of Cu(I). The kinetically stable adduct with
31 Pt(II) bridging the two proteins in the heterodimeric complex has also been structurally
32 characterized by X-ray crystallography. Together with the Pt(II)-bridged species (72% occupancy)
33 there is cocrystallization of a second species (28% occupancy) in which a Cu(I) is bound to Atox1
34 in a monodentate manner and to Mnk1 in a bidentate manner, this corresponds to one of the two
35 hypothesized Cu(I)-bridged forms of the functional heterodimer not yet characterized by X-ray
36 crystallography.

37
38 We propose that Pt drugs, apart from targeting DNA, can also impair Cu homeostasis with relevant
39 detrimental effect on the cellular viability and migration.

Fig. 1

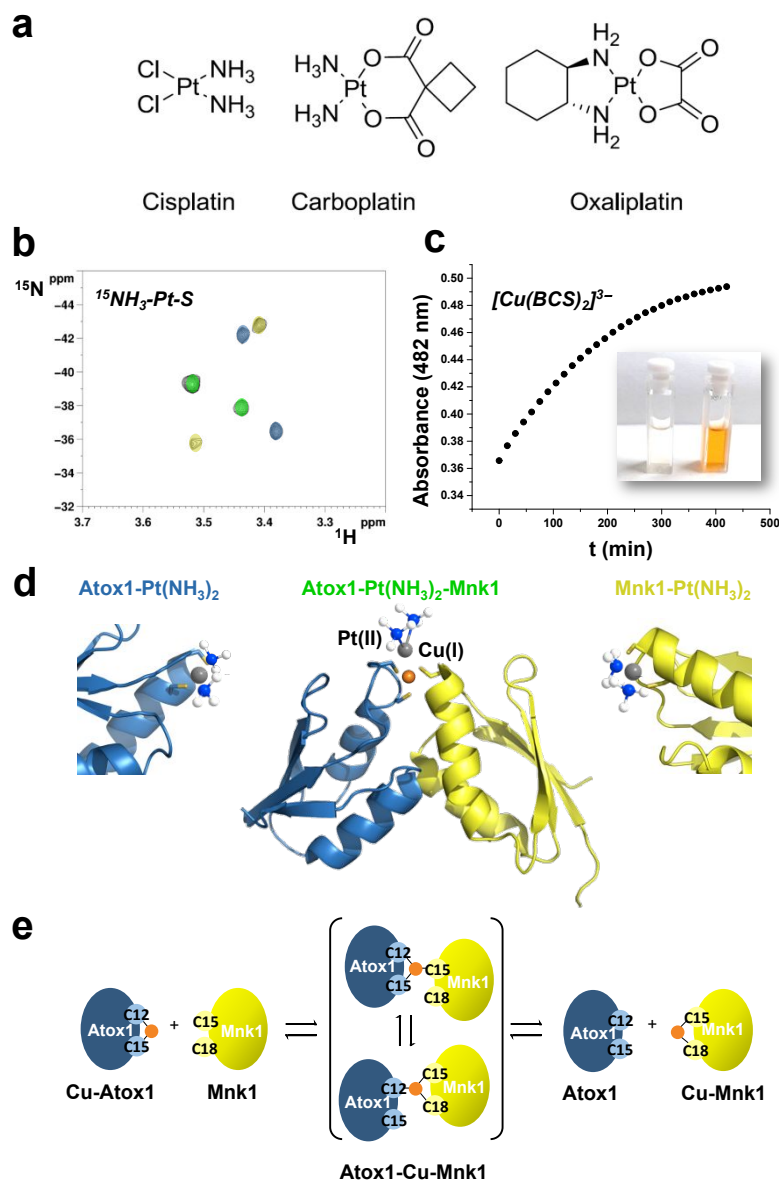


Figure 1. Cisplatin interferes with the rapid exchange of Cu(I) between the metallochaperone Atox1 and the first domain of Menkes ATPase (Mnk1). **a**, Chemical structures of Pt(II) anticancer drugs used in the clinics. **b**, Two-dimensional ^1H , ^{15}N -HSQC spectra of ^{15}N cisplatin incubated with Atox1-Cu(I)-Mnk1 complex for 4 h. Green cross-peaks belong to $^{15}\text{NH}_3$ of a platinated heterodimeric species, blue and yellow cross-peaks belong to $^{15}\text{NH}_3$ of monomeric bifunctional adducts of Atox1 and Mnk1, respectively. **c**, Time-dependent changes in absorbance at 482 nm ($[\text{Cu}^{\text{I}}(\text{BCS})_2]^{3-}$) following addition of ^{15}N cisplatin to the Atox1-Cu(I)-Mnk1 complex, with BCS present from the beginning of the incubation. The inset shows the color change of the solution

1
2
3 before addition of cisplatin and after 12 h incubation. **d**, Structural models of Atox1-Pt(NH₃)₂
4 (blue), Mnk1-Pt(NH₃)₂ (yellow) and heterodimeric Atox1-Pt(NH₃)₂-Mnk1 complex . Color codes:
5 gray = Pt, orange = Cu, blue = N, white = H. **e**, The three-coordinate mechanism of Cu(I) exchange
6 between Atox1 and Mnk1.
7
8
9
10
11
12
13
14
15
16
17
18
19
20
21
22
23
24
25
26
27
28
29
30
31
32
33
34
35
36
37
38
39
40
41
42
43
44
45
46
47
48
49
50
51
52
53
54
55
56
57
58
59
60

Results

Reaction of Atox1-Cu(I)-Mnk1 with cisplatin

In the presence of Cu(I), Atox1 and Mnk1 form a heterodimeric complex in solution which is in fast exchange with monomeric proteins⁴⁸; therefore, when ¹⁵N Cu(I)-Atox1 is titrated with increasing amounts of unlabeled apoMnk1 (up to one equivalent), in two-dimensional ¹H,¹⁵N Heteronuclear Single Quantum Coherence (HSQC) spectra only one set of signals is observed throughout the titration (Supporting Fig. 1). A similar behavior is observed when an analogous titration is performed starting from ¹⁵N Cu(I)-Mnk1 and adding aliquots of apoAtox1 (Supporting Fig. 2).

The weighted average chemical shift differences indicate that the most perturbed Atox1 residues belong to a positively charged patch that can interact with negative charges present on the surface of Mnk1 (Supporting Fig. 3); however, despite their surface complementarity, apoAtox1 and apoMnk1 do not form a complex in solution when mixed, indicating that the driving force to complex formation is provided by Cu(I) coordination to the CxxC consensus motifs of the two proteins⁴⁹. Notwithstanding the attomolar affinity for Cu(I)^{50,51} the complex is characterized by high kinetic lability⁵², which allows rapid (faster than milliseconds) exchange between complexed and free protein. The equilibrium is insensitive to Cu scavengers present in excess in the intracellular milieu⁵³ and, within the complex, the metal ion undergoes a facile switch between two coordination modes (two sulfur donor atoms from one protein and one sulfur from the other)^{6,54}; such a three-coordinate mechanism is also supported by NMR studies performed on Cu(I) complexes with GSH⁵².

To investigate the effect of cisplatin, two equivalents of ¹⁵N-labeled drug were added to the Atox1-Cu(I)-Mnk1 complex, under strict anaerobic conditions. The ¹⁵NH₃ chemical shifts of cisplatin are sensitive to the nature of donor atoms in *trans* position, therefore they can report changes in Pt coordination (the ¹⁵N nuclei of ammine ligands resonate approximately between -30 and -50 ppm when *trans* to S, between -50 and -75 ppm when *trans* to Cl or N, and between -70 and -90 ppm when *trans* to O)⁵⁵.

After 1 h incubation of ¹⁵N-labeled cisplatin with Atox1-Cu(I)-Mnk1, the ¹H,¹⁵N HSQC NMR spectrum in the region of ¹⁵NH₃ displayed new signals, in addition to those of the dichlorido (*cis*-[PtCl₂(¹⁵NH₃)₂], δ ¹⁵N ~ -67 ppm) and mono-aqua species (*cis*-[PtCl(¹⁵NH₃)₂(H₂O)]⁺, δ ¹⁵N ~ -66 and -83 ppm for ¹⁵NH₃ *trans* to Cl and O, respectively). Two cross-peaks were characteristic of ¹⁵NH₃ *trans* to S (δ ¹⁵N ~ -42.5 and -36.5 ppm) and were assigned to the bifunctional adduct Atox1-Pt(¹⁵NH₃)₂ with both cysteines of CxxC bound to Pt. Other two cross-peaks were assigned to the monofunctional adduct Mnk1-PtCl(¹⁵NH₃)₂ (δ ¹⁵N ~ -66 and -38 ppm for ¹⁵NH₃ *trans* to Cl and S,

1
2
3 respectively) (Supporting Fig. 4). The above peaks are similar to those observed in the reaction of
4
5 cisplatin with the free monomeric proteins^{44,45,56}.

6
7 After 4 h incubation, cross-peaks corresponding to the monofunctional adduct $\text{Mnk1-PtCl}(\text{}^{15}\text{NH}_3)_2$
8
9 converted into a new pair of cross-peaks ($\delta \text{}^{15}\text{N} \sim -43$ and -36 ppm) assigned to the bifunctional
10
11 adduct $\text{Mnk1-Pt}(\text{}^{15}\text{NH}_3)_2$ (Supporting Fig. 4). In the same spectrum, two new cross-peaks ($\delta \text{}^{15}\text{N}/^1\text{H}$
12
13 $-39/3.52$ and $-38/3.44$ ppm) appeared that were assigned to a Pt-bridged heterodimeric species with
14
15 both $^{15}\text{NH}_3$ ligands trans to S atoms (Fig. 1b). We will refer to the latter species as “upfield-shifted
16
17 Pt-bridged heterodimer”. Notably, the latter cross-peaks were never observed in the reactions of
18
19 cisplatin with the single proteins

20
21 After 12 h incubation, the $^{15}\text{NH}_3$ signals of the Pt derivatives with monomeric proteins vanished.
22
23 Also the cross-peaks of the upfield-shifted Pt-bridged heterodimer faded but were replaced by two
24
25 new signals, downfield-shifted along the proton dimension ($\delta \text{}^{15}\text{N}/^1\text{H} -48.5/3.90$ and $-45.5/4.07$
26
27 ppm, Supporting Fig. 4), which persisted even after 24 h of incubation. We will refer to the latter
28
29 species as “downfield-shifted Pt-bridged heterodimer”. The disappearance of the $^{15}\text{NH}_3$ signals of
30
31 the Pt derivatives with monomeric proteins could be due to protein unfolding, fostered by the
32
33 simultaneous binding of Cu and Pt to Atox1 or Mnk1^{39,44}, as witnessed by the coalescence of some
34
35 amide signals in the $^1\text{H},^{15}\text{N}$ HSQC spectrum (Supporting Fig. 5a,b).

36
37 Addition of bathocuproine disulfonate (BCS, a ligand which binds specifically Cu(I) to yield the 1:2
38
39 chromophoric complex $[\text{Cu}^{\text{I}}(\text{BCS})_2]^{3-}$ with high affinity ($\beta_2 = 10^{19.8} \text{ M}^{-2}$)⁵⁰) at the end of
40
41 incubation with cisplatin caused immediate disappearance of the downfield-shifted $^{15}\text{NH}_3$ signals
42
43 and reappearance of those of the initial upfield-shifted Pt-bridged heterodimer (Fig. 2a). Notably, a
44
45 similar behavior was observed when the physiological reducing agent GSH was added instead of
46
47 BCS (Fig. 2b). It can be concluded that the cross-peaks with deshielded ammine ligands ($\delta \text{}^{15}\text{N}/^1\text{H} -$
48
49 $48.5/3.90$ and $-45.5/4.07$ ppm) belong to a heterodimeric species containing a rather labile Cu
50
51 localized close to Pt.

52
53 When BCS was added at the onset of incubation, all $^{15}\text{NH}_3$ signals of monomeric Atox1 or Mnk1
54
55 bifunctional adducts were still detectable after 24 h, together with the signals of the upfield-shifted
56
57 Pt-bridged heterodimer, indicating that Cu(I) sequestration by BCS prevents both the formation of
58
59 the downfield-shifted Pt-bridged heterodimer and the degradation of the monomeric bifunctional
60
adducts (as also witnessed by the lack of signal coalescence in the protein HSQC spectrum,
Supporting Fig. 5c,d). In the latter experiment, UV-Vis absorption spectra showed a time-dependent
increase of absorbance at 482 nm due to formation of $[\text{Cu}^{\text{I}}(\text{BCS})_2]^{3-}$ (Fig. 1c), indicating a slow
release of Cu from the proteins to BCS (Fig. 1d).

1
2
3 The same reaction was further checked by HPLC/ESI-MS analysis. Thus, a mixture of holo ^{15}N
4 Atox1 and apoMnk1 was treated with two equivalents of cisplatin under strictly anaerobic
5 conditions at 25 °C and pH 7 (25 mM phosphate buffer). After 4 h incubation, the chromatogram
6 (UV detector) showed three main peaks with retention times (t_{R}) of 18.5, 19.2, and 19.6 min (Fig.
7 3a) whose mass spectra (Supporting Fig. 6) were in accord, in the order, with the following
8 compositions: ^{15}N Atox1-Pt(NH₃)₂ (7579 Da and 7710 Da), ^{15}N Atox1-Pt(NH₃)₂-Mnk1 (15947 Da
9 and 16078 Da), and ^{15}N apoAtox1 (7350 Da and 7481 Da) plus apoMnk1 (8368 Da). The first peak
10 in each deconvoluted spectrum corresponds to the expected total mass after cleavage of the N-
11 terminal methionine of Atox1 (131 Da).

12 The HPLC/ESI-MS spectrum of the peak at $t_{\text{R}} = 19.2$ min was further analyzed (Fig. 3b). Each
13 multi-charged state showed two main peaks, corresponding to ^{15}N Atox1-Pt(NH₃)₂-Mnk1 with or
14 without the N-terminal methionine of Atox1, and a series of low intensity signals corresponding to
15 ^{15}N Atox1-Pt(NH₃)₂-Mnk1 + 2Cu (16204 Da) and ^{15}N Atox1-Pt-Mnk1 + Cu (16107 Da, a
16 heterodimeric species in which Pt(II) has lost the amines). Thus, the HPLC/ESI-MS analysis
17 supports the co-presence of Cu(I) and Pt(II) also in the first formed heterodimeric complex with
18 upfield-shifted ammine protons.

19
20
21 According to the three-coordinate model of Cu(I) binding, only three cysteines of the two CxxC
22 motifs are needed for the formation of the Atox1-Cu(I)-Mnk1 complex (Fig. 1e)^{6,49}. While the two
23 cysteines that are more N-terminal in sequence (Cys12 of Atox1 and Cys15 of Mnk1) are strictly
24 required for the interaction, the third cysteine residue can be either Cys15 of Atox1 or Cys18 of
25 Mnk1⁴⁸.

26 We used site-directed mutagenesis of the latter two residues to investigate the role of individual
27 cysteines in the formation of adducts with cisplatin. Upon addition of two equivalents of ^{15}N -
28 labeled cisplatin to a 1:1 mixture containing the WT form of one protein and the mutant of the other
29 protein (lacking the cysteine less N-terminal in sequence), the NMR spectra showed that in both
30 cases (Atox1-Cu(I)-C18A Mnk1 and C15A Atox1-Cu(I)-Mnk1) only a platinated heterodimeric
31 species was formed, while no peaks related to monomers could be detected (Supporting Figs. 7 and
32 8). The $^{15}\text{NH}_3$ signals were sensitive to the addition of BCS, giving rise, in both cases, to a new pair
33 of upfield-shifted signals (Fig 2a). Thus, unlike the case of wild-type proteins, in the case of
34 mutants the formation of the heterodimeric species with downfield shifted ammine signals is
35 observed from the beginning. Interestingly, the reaction with cisplatin was faster in the case of
36 Atox1-Cu(I)-C18A Mnk1 than in the case of C15A Atox1-Cu(I)-Mnk1. Finally, when both mutants
37
38
39
40
41
42
43
44
45
46
47
48
49
50
51
52
53
54
55
56
57
58
59
60

were mixed together, no adducts were formed, consistent with the fact that one cysteine from each protein is not sufficient to stabilize the Atox1-Cu(I)-Mnk1 heterodimer.

SDS-PAGE, performed at the end of incubation with cisplatin, showed that in all cases (WT proteins and mutants), a dimeric species resistant to the denaturing conditions of the gel was present (Fig. 2c), which is most likely supported by a Pt bridge as witnessed by the characterization of Pt(II)-supported heterodimeric species by NMR and X-ray crystallography and the absence of heterodimeric complex resistant to denaturing gel in the absence of added Pt drug.

Fig. 2

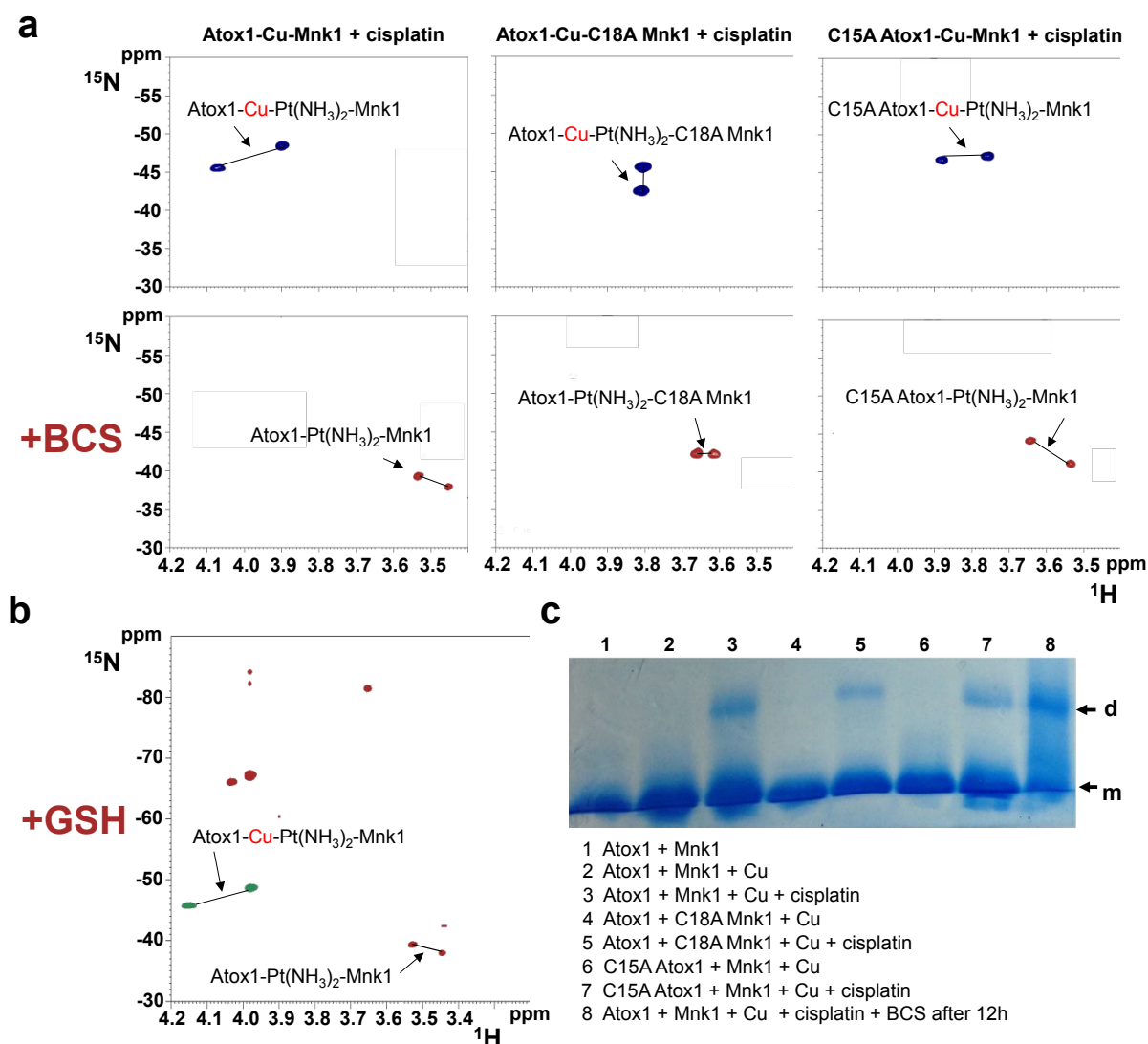


Figure 2. Binding of cisplatin stabilizes heterodimers of Atox1 and Mnk1. **a**, Two-dimensional ^1H , ^{15}N -HSQC spectra of ^{15}N cisplatin incubated for 24 h with Atox1-Cu(I)-Mnk1, Atox1-Cu(I)-C18A Mnk1 and C15A Atox1-Cu(I)-Mnk1 complexes, before and after addition of bathocuproine

1
2
3 disulfonate (BCS); the formulae include only the labile Cu which is shown in red. **b**, Overlay of
4 two-dimensional ^1H , ^{15}N -HSQC spectra of ^{15}N cisplatin incubated for 24 h with Atox1-Cu(I)-Mnk1
5 complex, before (green contours) and after (brown contours) addition of glutathione (GSH); the
6 formulae include only the labile Cu which is shown in red. **c**, SDS-PAGE of various samples
7 incubated in the absence or in the presence of cisplatin, as indicated in the legend for lanes 1-8. The
8 positions of protein monomers (m) and heterodimers (d) resistant to denaturing gel conditions are
9 indicated by arrows.

10
11
12
13
14
15
16
17 *The Pt-bridged heterodimeric species does not form if transplatin is used in place of cisplatin or*
18 *Zn(II) is used in place of Cu(I)*

19
20 For an unspecific bridging interaction, transplatin is expected to behave similarly to cisplatin,
21 therefore an experiment was performed in which transplatin was added to a solution of the
22 preformed Atox1-Cu(I)-Mnk1 complex. Although Atox1 exhibited some reactivity toward
23 transplatin (a Pt-bound Atox1 was detected by HPLC/ESI-MS analysis), no peaks assignable to Pt-
24 bridged dimeric species were detected (Supporting Fig. 9). Therefore, the *cis* orientation of the
25 leaving ligands in the Pt substrate is essential for cross-linking Atox1 and Mnk1.

26
27
28
29 The results so far obtained also indicate that a preformed Atox1-Cu(I)-Mnk1 heterodimer is
30 required for the formation of a Pt-containing heterodimeric species. To check whether the
31 preformed Atox1-Mnk1 heterodimer must have a specific conformation, we performed an
32 experiment in which cisplatin was added to a solution in which the two proteins had been incubated
33 with Zn(II) (known to be able to bridge the two proteins)⁵¹.

34
35
36
37
38
39
40
41
42
43
44
45
46
47
48
49
50
51
52
53
54
55
56
57
58
59
60
SDS-PAGE and HPLC/ESI-MS analysis revealed that, under the above conditions, only Pt-
containing monomeric species were formed, while there was no indication, whatsoever, of
formation of Pt-containing heterodimeric species (Supporting Fig. 10). The NMR investigation also
showed that the reaction of cisplatin with the Atox1-Zn(II)-Mnk1 complex is very slow and leads to
two sets of signals ($\delta^{15}\text{N} \sim -84/-83$ and -41 ppm for $^{15}\text{NH}_3$ trans to O and S, respectively), identical
to those obtained by reaction of cisplatin with Zn(II)-Atox1 in the absence of Mnk1 (Supporting
Figs. 11 and 12), thus indicating that, in the presence of Zn(II), cisplatin selectively binds to the
Atox1 monomer. It is concluded that the use of Cu(I) is a harbinger of the Atox1-Pt(NH₃)₂-Mnk1
complex formation.

56
57
58
59
60
Crystal structure of the Pt-bridged heterodimeric species with trapped Cu(I) ion

To gain an atomistic view of the Pt-bridged heterodimeric species, a crystallographic investigation
was undertaken. Since the long-time (some days) required for crystallization experiments can foster

1
2
3 the loss of the ammine ligands, we used an aquated form of oxaliplatin (*cis*-[Pt(SO₄)(H₂O)(1,2-*R,R*-
4 DACH)]) (DACH = diaminocyclohexane) containing a chelated, and intrinsically less labile ⁵⁷,
5 diamine ligand (see Supporting *Materials and Methods*). First, it was proven that aquated
6 oxaliplatin behaves as cisplatin, affording the analogous Pt-bridged heterodimeric species in which
7 Pt retains the DACH ligand (Supporting Fig. 13).
8
9

10 After incubation of the Atox1-Cu(I)-Mnk1 complex with two equivalents of *cis*-[Pt(SO₄)(H₂O)(1,2-
11 *R,R*-DACH)] and detection of the Atox1-Pt(1,2-*R,R*-DACH)-Mnk1 heterodimeric species by ESI-
12 MS, the hanging drop technique was used to produce rod crystals having P 2₁2₁2₁ symmetry. The
13 structure (PDB entry 5T7L) was solved to a resolution of 2.8 Å (unit cell parameters and diffraction
14 data statistics are shown in Supporting Table 1).
15
16

17 The asymmetric unit contains the two protein molecules (Atox1 is chain A, Mnk1 is chain B)
18 arranged around a non-crystallographic 2-fold axis (Fig. 3c). The overall arrangement is similar to
19 that of the heterodimer crystallized in the presence of Cd(II) (PDB entry 3CJK, 1.8 Å resolution) ⁴⁸,
20 with an overall *C α* root-mean-square deviation (RMSD) of only 0.73 Å (RMSD of 0.37 Å for chain
21 A and 0.84 Å for chain B).
22
23
24
25
26
27
28
29

30 *Platinum binding sites*

31 The Pt atoms have been clearly identified by using the anomalous signal (data collection was
32 performed at 11700 eV, just above the Pt L3 edge), while the presence of Cu atoms was assessed
33 based on the electron density map height (very weak Cu anomalous signal is expected at the above
34 energy). Two Pt-binding sites are present, the 2Fo-Fc electron density map (in grey) and the
35 anomalous map (in magenta) around the two Pt ions are shown in Fig. 3d.
36
37
38

39 In the first site the Pt ion (Pt1 in Fig. 3d) is bound to two cysteine residues: Cys12 of chain A and
40 Cys15 of chain B. The two S atoms are, respectively, at a distance of 2.8 and 2.3 Å from Pt1 and
41 form an S-Pt-S angle of 86.0° (details on bond distances and angles are given in Supporting Tables
42 2 and 3). Apart from the two cysteine residues, no other molecule, protein residue, or ion was found
43 close to the Pt center, notwithstanding the starting Pt substrate contained a chelating DACH ligand.
44 The high atomic displacement factor of Pt1 (*B* = 93.1 Å²) may indicate a static disorder of the site,
45 which hinders the detection of the Pt ligands in the solvent exposed region opposite the two bound
46 cysteines; however the S-Pt-S angle of 86.0° clearly supports a square-planar coordination for the Pt
47 center. Second shell reconstructed atoms are: W7 (4.6 Å); N of Cys12 (4.3 Å) and Cys15 (4.6 Å)
48 and OG1 of Thr14 (4.8 Å) for chain B; N of Gly13 (4.7 Å) and O of Thr11 (4.9 Å) for chain A. The
49 second Pt-binding site (Fig. 3d), located close to Cys41 of chain A (Atox1), will be discussed at the
50 end of this section.
51
52
53
54
55
56
57
58
59
60

1
2
3 In the region of the two CxxC motifs, besides the Pt1 ion, there are also two Cu ions at 6.0 Å (Cu1)
4 and 3.9 Å (Cu2) distance from Pt1 (Fig. 3d). Cu1 is in approximate linear coordination with the
5 sulfur atoms of Cys15 of chain A (2.2 Å) and Cys18 of chain B (2.3 Å) forming a S-Cu-S angle of
6 166.7°. Unlike Cu1, Cu2 is very close to the position of the Cd(II) ion in the Atox1-Cd(II)-Mnk1
7 complex (3CJK model)⁴⁸. This latter finding, coupled with the consideration that a distance of only
8 3.9 Å between Cu2 and Pt1 would lead to local electrostatic instability, lead us to hypothesize two
9 alternate configurations for this heterodimer: one configuration comprising Pt1 and Cu1 and the
10 other configuration comprising Cu2, this latter having a coordination very similar to that of Cd(II)
11 in 3CJK. As a consequence, we split Cys12 and Cys15 of chain A and Cys15 of chain B in two
12 conformations, one conformation corresponding to that refined from our data, the other
13 conformation corresponding to that present in 3CJK. It is worth noting that for Cys18 of chain B the
14 conformation refined from our data coincides with that present in 3CJK. Thus, Cu2 has a distorted
15 tetrahedral coordination which involves S γ of Cys12 (2.2 Å) for chain A and S γ of Cys15 (2.6 Å)
16 and Cys18 (2.9 Å) and O γ 1 of Thr14 (2.8 Å) for chain B. The crystallographic occupancies of the
17 metal ions and corresponding donor atoms resulted to be 0.72 for the Pt1-Cu1 configuration, and
18 0.28 for the Cu2 one.
19

20
21
22 The second Pt-binding site (Fig. 3d) is located close to Cys41 of chain A (Atox1). This Pt ion
23 (crystallographic occupancy of 0.36) is coordinated by the S atom of Cys41 (2.7 Å) and the N ζ
24 atom of Lys3 (2.7 Å) of chain A. Two water molecules complete a distorted square-planar
25 coordination geometry (average Pt-O distance of 2.7 Å). This site has a similarity with that recently
26 found for the Atox1 homodimer crystallized in analogous conditions (PDB entry 4QOT)⁵⁸.
27 However, the Lys3 side chain assumes a different conformation in the heterodimer as compared to
28 the Atox1 homodimer so that, after superposition of the Atox1 chains, the Pt2 atoms are 3.5 Å far
29 apart.
30

31 *Noncovalent interactions*

32
33 Two salt bridges (Asp68B-Arg21A and Glu11B-Lys42B) are in common with the 3CJK model
34 (Cd(II) heterodimer), while the two additional Asp9A-Lys60A and Asp63B-Lys25A salt bridges
35 (the latter also forming an H-bond) replace the salt bridge Glu43A-Lys3A present in 3CJK, which
36 has been disrupted by the reorientation of the Pt2-bound Lys3A side chain.
37

38 Although the overall number of H-bonds was greater in the 3CJK model, the present structure,
39 5T7L, exhibits two additional intra-dimer interactions with new Cys12A-Thr14B and Gly14A-
40 Thr14B H-bonds fostered by the reorientation of the metal-bound residues Cys12A and Thr14B.
41
42
43
44
45
46
47
48
49
50
51
52
53
54
55
56
57
58
59
60

Overall, the larger number of intra-dimer noncovalent interactions stabilizes the 5T7L heterodimer, which assumes a more closed configuration than the 3CJK heterodimer.

Fig. 3

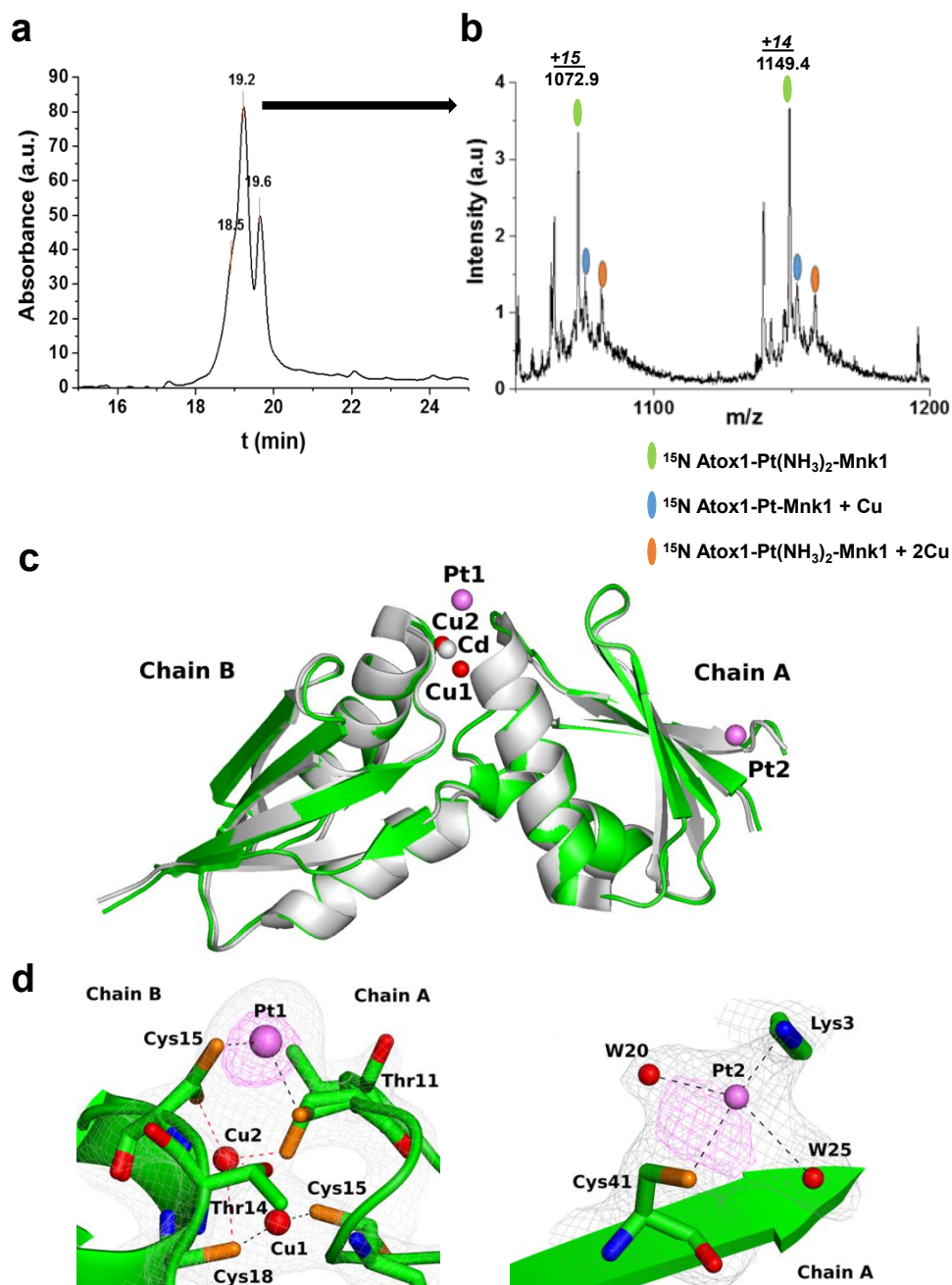


Figure 3. Stoichiometry and crystal structure of platinated heterodimers of Atox1 and Mnk1.

a, HPLC-UV chromatogram of ^{15}N Atox1-Cu(I)-Mnk1 complex incubated for 4 h with two equivalents of cisplatin. **b**, HPLC/ESI-MS spectrum of the peak eluted at $t_{\text{R}} = 19.2$ min; only the two

1
2
3 most intense multi-charged states are displayed and the assigned peaks are labeled with ovals. **c**,
4 Crystal structure of the heterodimeric complex (green) crystallized in the presence of
5 [Pt(SO₄)(H₂O)(1,2-*R,R*-DACH)], superimposed to that of the Atox1-Cd(II)-Mnk1 complex (light
6 gray, PDB entry 3CJK). Atox1 (chain A) and Mnk1 (chain B) molecules are shown in cartoon
7 representation. Pt, Cu and Cd atoms are shown as magenta, red, and gray spheres, respectively. **d**,
8 Platinum binding sites Pt1 and Pt2. Protein residues within 3 Å from Pt and Cu are shown as sticks,
9 with C, O, N, and S atoms colored in green, red, blue, and yellow, respectively. The 2Fo-Fc
10 electron density map (grey, 2σ for Pt1 and 1σ for Pt2 sites) and the anomalous map (magenta, 6σ
11 for Pt1 and 3σ for Pt2 sites) are also shown. Dashed lines are drawn between the metal ions and the
12 closest protein donor atoms. Red and black dashed lines indicate the two different metallic cores
13 (one comprising Pt1 and Cu1 and the other Cu2) of the crystallized heterodimer.
14
15
16
17
18
19
20
21
22
23
24
25
26
27
28
29
30
31
32
33
34
35
36
37
38
39
40
41
42
43
44
45
46
47
48
49
50
51
52
53
54
55
56
57
58
59
60

Discussion

Previous studies have shown that Atox1 is able to bind to Pt in a bidentate manner forming the species Atox1-Pt(NH₃)₂^{46,56}; in contrast, Mnk1 first generates the monofunctional adduct Mnk1-PtCl(NH₃)₂, which subsequently evolves towards the bidentate species Mnk1-Pt(NH₃)₂⁴⁴.

In the presence of GSH, Atox1 does not compete successfully with the physiological thiol for Pt binding; in contrast, Mnk1 does coordinate to Pt⁴⁵. Remarkably, preloading with Cu enhances the reactivity of both proteins toward cisplatin: Cu(I)-Atox1 readily coordinates Pt even in the presence of GSH and Cu(I)-Mnk1 gives directly the bifunctional adduct Mnk1-Pt(NH₃)₂^{44,45}. Increased platination rate, as a consequence of preloading with copper, has also been demonstrated for other soluble domains of Atp7a and Atp7b⁴⁷.

In competition experiments, cisplatin reacts with Mnk1 in preference to Atox1⁴⁵; however, Pt-loaded Atox1 is unable to handover Pt to Mnk1.

A reactivity non ascribable to that of the single proteins is observed in the case of reaction of cisplatin with the Atox1-Cu(I)-Mnk1 heterodimeric complex.

Reaction of cisplatin with wild-type proteins

In the case of wild-type proteins the heterodimeric complex Atox1-Cu(I)-Mnk1 is in equilibrium with the monomeric species^{48,54}. In the first hour of incubation only Pt-adducts of monomeric proteins are formed; however, while monomeric Atox1 gives the bifunctional adduct Atox1-Pt(NH₃)₂ notwithstanding the presence of Mnk1, monomeric Mnk1, similarly to the case of absence of Cu, forms first the monodentate Mnk1-PtCl(NH₃)₂ adduct that only afterwards affords the bidentate Mnk1-Pt(NH₃)₂ species. The latter results can be explained by looking at the solution structure of the Cu(I)-mediated complex between the yeast homologues of Atox1 and Mnk1 (Atx1 and the first domain of Ccc2 ATPase)⁴⁹. In the Cu(I)-mediated heterodimeric complex Atx1 was found to have a conformation more similar to its monomeric Cu(I)-loaded state (helix α 1 fully formed and Cys15 in helical conformation, at variance with the *apo* state), which would favor the formation of a bifunctional adduct with cisplatin. In contrast, the ATPase domain was found to undergo a conformational rearrangement with partially unwound helix α 1, which would disfavor the formation of the bifunctional adduct with cisplatin. Thus, the conformational changes observed in the yeast homologues are consistent with the observed reactivity toward cisplatin of human proteins when in a complex with a bridging Cu(I) ion, i.e. Atox1 reacts as in its Cu(I)-bound form while Mnk1 reacts as in its *apo* form.

Unlike the case of mutants (see following discussion), the initially formed Atox1-Pt(NH₃)₂-Mnk1 heterodimeric complex (at 4 h incubation time) has upfield-shifted ¹⁵NH₃ signals, and only at longer

1
2
3 reaction time (after 12 h incubation) it undergoes transition to a downfield-shifted Pt-bridged
4 heterodimer containing a labile Cu that can be rapidly removed by BCS or GSH giving back the
5 first formed heterodimeric complex with upfield-shifted $^{15}\text{NH}_3$ signals. The initial formation of the
6 upfield-shifted Pt-bridged heterodimer in the case of the wild-type proteins may reflect the
7 increased metal-loading capacity of the four thiolate ligands which, after coordination of Pt(II) to
8 the more N-terminal cysteines of the CxxC motifs, can retain the Cu(I) ion in an internal/buried site
9 involving the less N-terminal cysteines (Cys15 of Atox1 and Cys18 of Mnk1). This possibility is
10 excluded in the case of one wild-type protein and one mutant, due to the lack of the second internal
11 cysteine. With time some Cu can be taken up from the solution by the initially formed heterodimer
12 yielding the downfield-shifted Pt-bridged heterodimer containing a labile Cu close to Pt which, if
13 removed by BCS, gives back the initial upfield-shifted Pt-bridged heterodimer.

14
15 Most likely, the downfield-shifted Pt-bridged heterodimeric complex cannot form in physiological
16 conditions due to the presence of GSH, which has been shown to be able to remove the labilized
17 Cu.

18
19 Interestingly, both the nature of the pre-loaded metal ion (Cu(I)) and the *cis* configuration of the Pt
20 substrate are required for the formation of the Pt-bridged heterodimeric complex, a clear example of
21 metal template specificity. Indeed, by using Zn(II) in place of Cu(I) and transplatin in place of
22 cisplatin no Pt-bridged heterodimeric species was formed. This specific recognition of the Atox1-
23 Cu(I)-Mnk1 heterodimer by *cis*-oriented Pt(II) complexes is rather peculiar and not envisaged up to
24 now.

25
26 Concerning the absence of interprotein cross-link when transplatin was used instead of cisplatin, we
27 recall that both the intermolecular interactions and the metal ion bridging the two proteins
28 contribute to the stability of heterodimeric adducts ^{48,49}. It is likely that the two more N-terminal
29 cysteines are suited for a *cis*-coordination to platinum rather than for a *trans*-coordination as
30 required by the *trans* isomer. Due to steric reasons, transplatin is also unable to form 1,2-intrastrand
31 cross-links between two adjacent purines on a DNA strand, and this was related to its lack of
32 pharmacological activity ²¹.

33
34 Concerning the different behavior of the Cu(I)- and Zn(II)-supported heterodimers, the results of the
35 present investigation show that even in the case of Cu(I), which can assume two different
36 configurations in the Atox1-Cu-Mnk1 heterodimer, one configuration (monofunctional Atox1 and
37 bifunctional Mnk1) is less reactive towards Pt than the other (bifunctional Atox1 and
38 monofunctional Mnk1). This implies the necessity of a fine matching between the preformed
39 heterodimer (with either Cu(I) or Zn(II) bridging ion) and the attacking Pt substrate; most likely
40 Zn(II) cannot provide such a fine matching.

Reaction of cisplatin with mutated proteins

The reaction of ^{15}N -labeled cisplatin with a 1:1 mixture containing the WT form of one protein and the mutant of the other protein (either C15A Atox1 or C18A Mnk1) leads to the direct and exclusive formation of a Pt-bridged heterodimeric complex with downfield-shifted $^{15}\text{NH}_3$ signals from which a Cu(I) ion can be rapidly removed by BCS leading to a Pt-bridged heterodimeric complex with upfield-shifted $^{15}\text{NH}_3$ signals. The absence of Pt adducts with monomeric proteins, suggests that the lack of a cysteine in one partner shifts the equilibrium completely towards the Cu(I)-bridged heterodimeric form, which has no tendency to dissociate into monomers. Moreover, the immediate formation of the Pt-heterodimeric complex with downfield-shifted $^{15}\text{NH}_3$ signals indicates that the pre-loaded Cu(I) ion cannot be retained buried inside (as in the case of wild-type proteins) due to the presence of only one internal cysteine, therefore this Cu(I) ion is immediately available for colocalization near the Pt atom. Finally, the greater reactivity toward cisplatin of Atox1-Cu(I)-C18A Mnk1 with respect to C15A Atox1-Cu(I)-Mnk1 could stem from a different solvent accessibility as well as from a different ability to reorient the two cysteines that bind to Pt (each protein contributes only one cysteine sulfur to Pt, the more N-terminal cysteine of the CxxC motifs, with the two amines completing the square planar coordination geometry).

X-ray structure of the wild-type heterodimeric species

The crystallization of a Pt-containing heterodimeric species provided a unique opportunity to gain structural insights also into the elusive Cu-bridged forms.

The analysis of the crystalline structure pointed to the coexistence of two species. In one species a Cu atom (Cu2) is bound to Atox1 in a monodentate manner and to Mnk1 in a bidentate manner (which corresponds to one of the two hypothesized Cu(I)-bridged forms of the functional heterodimer). This Cu coordination mode, which has never been structurally characterized before, corresponds to that found in the Cd(II)-bridged heterodimer previously reported⁴⁸. Such a Cu(I) coordination should be the only one admitted in the C15A Atox1-Cu(I)-Mnk1 mutant, which has been found to be scarcely reactive toward Pt(II). The second hypothesized Cu(I)-bridged form of the functional heterodimer has Cu(I) bound to Atox1 in a bidentate manner and to Mnk1 in a monodentate manner. This latter coordination should be the only one admitted in the Atox1-Cu(I)-C18A Mnk1 mutant, which has been found to be more reactive toward Pt(II). Indeed, looking at the arrangement of thiols in Fig. 3d, it can be guessed that Cys15 of Mnk1 and Cys12 and Cys15 of Atox1 are less suited to three-coordinate a Cu(I) ion, therefore the corresponding heterodimer is expected to be more reactive toward Pt(II). This explains why the conformation with monodentate

1
2
3 Atox1 and bidentate Mnk1 (being intrinsically more stable) has been observed in the solid state for
4 both Cu(I) (Cu2 in the present investigation) and Cd(II). Importantly, apart from the structural
5 considerations made above, the experiments performed with mutated proteins have shown that, of
6 the two possible binding configurations of the Cu(I) ion in the cage made by the CxxC motifs of the
7 two proteins, one (bidentate Atox1 and monodentate Mnk1) is more reactive towards cisplatin and
8 hence less stable than the other.
9

10 In the second species present in the crystal structure, a Pt atom (Pt1) is bound to the more N-
11 terminal cysteines of Atox1 and Mnk1 and a Cu atom (Cu1) is bound to the internal cysteines of the
12 same proteins. It can be hypothesized that, after coordination of Pt to the more exposed cysteines,
13 the Cu(I) ion is pushed down reaching a new energy minimum. The observation in the ESI-MS
14 spectra of heterodimeric fragments containing both Pt and Cu points to a good stability of the
15 second species present in the crystal structure. In this heterodimeric complex the NMR signals of
16 the amines bound to Pt would not be affected by the presence of the buried Cu(I) ion, due to the
17 large Cu-Pt distance ($> 6 \text{ \AA}$), therefore the initially formed heterodimeric complex has upfield-
18 shifted $^{15}\text{NH}_3$ signals, and only at longer reaction time it undergoes transition to a downfield-shifted
19 Pt-bridged heterodimer. In contrast, in the case of mutants the presence of only one internal cysteine
20 does not allow such an internal stabilization of the Cu(I) ion, as a consequence the Pt-bridged
21 heterodimer formed right from the beginning contains downfield-shifted $^{15}\text{NH}_3$ signals and a labile
22 Cu that can be rapidly removed by BCS. This fully explains the different behavior of wild-type and
23 mutated heterodimers.
24
25
26
27
28
29
30
31
32
33
34
35
36
37
38

39 *Biological implications of platinum binding to dithiol motifs of copper proteins*

40 Pull-down experiments in yeast cells have shown that cisplatin binds to CxxC motifs of Atox1 and
41 protein disulfide isomerases (PDI), thereby inhibiting their function and ultimately resulting in the
42 induction of endoplasmic reticulum stress⁵⁹. Moreover, in a yeast two-hybrid screen using Atox1 as
43 bait, many of the proteins found to be confident interaction partners contain CxxC motifs, indicating
44 that interactions between these and Atox1 can also be mediated by Cu⁶⁰. In the light of the present
45 investigations, all these processes are keen to be disrupted by cisplatin.
46
47
48
49

50 Cisplatin treatment also causes a significant increase (doubling) of ROS levels¹². Mechanistically,
51 this may be a consequence of thiol blockage and metal dishomeostasis. Unlike the kinetically labile
52 and exchangeable Cu(I) ion, Pt(II) acts as an efficient thiol scavenger as it irreversibly modifies the
53 two-cysteine motifs and, by blocking the redox-sensitive thiol groups, contributes to oxidative
54 stress. While an anticancer therapy that favors ROS accumulation may be more effective in
55 inducing programmed cell death⁶¹, a rise in intracellular Cu, consequent to a blockage of Cu efflux
56
57
58
59
60

1
2
3 machinery, can lead to increased levels of Cu-ATPases, which in turn cause enhanced drug
4 sequestration and resistance to Pt chemotherapy. Thus, Pt drugs, by impacting Cu transport, can
5 induce their own resistance. The arrangement of all six N-terminal MBDs of Menkes ATPase is
6 regulated by Cu and controls the intracellular localization and catalytic activity of the pump^{3,62}. The
7 Pt ability to cross-link Atox1 and Mnk1 suggests that tethering Atox1 to Atp7a soluble domains
8 may compromise the Cu(I)-mediated trafficking of Menkes ATPase to the plasma membrane, while
9 Pt may become stuck between the proteins.

10 Such a mechanism of Pt cross-linking can be extended to other MBDs of Cu-ATPases and their Cu-
11 dependent complexes with Atox1 and other proteins containing the dithiol motif. For instance,
12 lysosomal exocytosis and Cu clearance are regulated by the Cu-dependent interaction between
13 MBD6 of Wilson ATPase and the p62 subunit of dynactin⁶³, both containing a CxxC motif^{64,65}.
14 Binding to p62 allows Atp7b-containing membranes to anchor the dynein motor and, therefore, to
15 be translocated to the biliary surface.

16 By binding to N-terminal MBDs of Cu-ATPases, Pt drugs can also alter their overall arrangement
17 and recognition by the protein translocation machineries. Changes in the subcellular localization of
18 Cu-ATPases can facilitate sequestration of cisplatin in vesicular structures of the endosomal
19 pathway^{40,43}, which may prevent drug binding to genomic DNA, thereby contributing to cisplatin
20 resistance and chemotherapy failure⁶⁶. Moreover, thiol modifications have important implications
21 also for the mechanism of extracellular vesicle release⁶⁷.

22 Based on these findings, cisplatin, rather than being just a cargo for Cu transporters, can interfere
23 deeply with Cu transport and metabolism. Interestingly, the co-administration of Pt drug and a Cu
24 chelator, such as tetrathiomolybdate (TM), can increase the nuclear availability of cisplatin and
25 resensitize resistant cells⁶⁸. TM was shown to inhibit the reaction of cisplatin with Cu-Atox1⁶⁹ by
26 forming a Mo-centered trimeric protein cluster with trapped Cu ions⁷⁰. Similarly, the reaction of Pt
27 drugs with MBDs of Cu-ATPases is fostered by Cu ions. Finally, the present investigation has
28 shown that also Pt bridging of Atox1 to MBDs of Cu-ATPases requires the presence of Cu.

29 **Conclusion**

30 In conclusion, *cis*-Pt(II) compounds, which are among the most used chemotherapeutics, have the
31 ability to bind CxxC motifs and form interprotein cross-links between the Cu chaperone Atox1 and
32 the N-terminal domains of Menkes ATPase, thus hindering the release of Cu to cuproenzymes and
33 the efflux of excess Cu from the cell. Indeed, increased copper content has been observed in human
34 cancer cells after cisplatin treatment^{71,72}. Interestingly, the Pt-bridged heterodimeric species does
35 not form if transplatin is used in place of cisplatin or Zn(II) is used in place of Cu(I). The kinetically
36
37
38
39
40
41
42
43
44
45
46
47
48
49
50
51
52
53
54
55
56
57
58
59
60

1
2
3 stable Pt(II)-bridged adduct has also been characterized by X-ray crystallography. Together with the
4 Pt(II) bridged species (72% occupancy) there is cocrystallization of a second species (28%
5 occupancy) in which a Cu(I) is bound to Atox1 in a monodentate manner and to Mnk1 in a
6 bidentate manner, this corresponds to one of the two hypothesized Cu(I)-bridged forms of the
7 functional heterodimer not yet characterized by X-ray crystallography. The same conformer has
8 been shown, through studies of site-directed mutagenesis, to be more stable and less reactive
9 towards Pt(II) than the second conformer comprising bidentate Atox1 and monodentate Mnk1.
10 After Pt(II) coordination, a Cu(I) ion can still be retained at the metal-binding site, but it is labilized
11 and can be released to glutathione (a physiological thiol) or to other complexing agents.
12 Conclusively, Pt drugs, apart from targeting DNA, can also impair Cu homeostasis by interfering
13 with the rapid exchange of Cu(I) between Atox1 and Cu-ATPases with relevant detrimental effect
14 on the cellular viability and migration.
15
16
17
18
19
20
21
22
23
24

25 **Associated Content**

26 *Supporting Information*

27 The Supporting Information is available free of charge on the ACS Publications website.

28 Experimental details, additional NMR experiments, HPLC/ESI-MS spectra and crystallographic
29 data. The structure of Pt-containing Atox1-Cu(I)-Mnk1 heterodimer has been deposited in the
30 Protein Data Bank as entry 5T7L.
31
32
33
34
35
36

37 **Acknowledgments**

38 This work was supported by the Italian Ministero dell'Istruzione, dell'Università e della Ricerca
39 (PONA3_00395 "Bioscience & Health"), the University of Bari and the Consorzio Interuniversitario
40 di Ricerca in Chimica dei Metalli nei Sistemi Biologici (CIRCMSB). The authors thank the
41 European Synchrotron Radiation Facility for providing access to beamline ID23-1, the Diamond
42 Light Source for providing access to beamline I02, Prof. Francesco Paolo Intini for assistance in the
43 synthesis of platinum complexes and Francesco Cannito for technical assistance in ESI-MS and
44 AAS measurements.
45
46
47
48
49
50
51
52
53
54
55
56
57
58
59
60

References

- (1) Hung, I. H.; Casareno, R. L. B.; Labesse, G.; Mathews, F. S.; Gitlin, J. D. HAH1 Is a Copper-Binding Protein with Distinct Amino Acid Residues Mediating Copper Homeostasis and Antioxidant Defense. *J. Biol. Chem.* **1998**, *273* (3), 1749–1754.
- (2) Lutsenko, S.; Petrukhin, K.; Cooper, M. J.; Gilliam, C. T.; Kaplan, J. H. N-Terminal Domains of Human Copper-Transporting Adenosine Triphosphatases (the Wilson's and Menkes Disease Proteins) Bind Copper Selectively in Vivo and in Vitro with Stoichiometry of One Copper per Metal-Binding Repeat. *J. Biol. Chem.* **1997**, *272* (30), 18939–18944.
- (3) Banci, L.; Bertini, I.; Cantini, F.; Della-Malva, N.; Migliardi, M.; Rosato, A. The Different Intermolecular Interactions of the Soluble Copper-Binding Domains of the Menkes Protein, ATP7A. *J. Biol. Chem.* **2007**, *282* (32), 23140–23146.
- (4) Banci, L.; Bertini, I.; Cantini, F.; Massagni, C.; Migliardi, M.; Rosato, A. An NMR Study of the Interaction of the N-Terminal Cytoplasmic Tail of the Wilson Disease Protein with Copper (I)-HAH1. *J. Biol. Chem.* **2009**, *284* (14), 9354–9360.
- (5) Arnesano, F.; Banci, L.; Bertini, I.; Ciofi-Baffoni, S.; Molteni, E.; Huffman, D. L.; O'Halloran, T. V. Metallochaperones and Metal-Transporting ATPases: A Comparative Analysis of Sequences and Structures. *Genome Res.* **2002**, *12* (2), 255–271.
- (6) Rosenzweig, A. C.; Wernimont, A. K.; Huffman, D. L.; Lamb, A. L.; O'Halloran, T. V. Structural Basis for Copper Transfer by the Metallochaperone for the Menkes/Wilson Disease Proteins. *Nat. Struct. Biol.* **2000**, *7* (9), 766–771.
- (7) Culvenor, J. G.; Lockhart, P.; Gleeson, P. A.; Mercer, J. F.; Camakaris, J.; Petris, M. J. Ligand-Regulated Transport of the Menkes Copper P-Type ATPase Efflux Pump from the Golgi Apparatus to the Plasma Membrane: A Novel Mechanism of Regulated Trafficking. *EMBO J.* **1996**, *15* (22), 6084–6095.
- (8) Hamza, I.; Prohaska, J.; Gitlin, J. D. Essential Role for Atox1 in the Copper-Mediated Intracellular Trafficking of the Menkes ATPase. *Proc. Natl. Acad. Sci.* **2003**, *100* (3), 1215–1220.
- (9) Denoyer, D.; Masaldan, S.; La Fontaine, S.; Cater, M. A. Targeting Copper in Cancer Therapy: 'Copper That Cancer.' *Metallomics* **2015**, *7* (11), 1459–1476.
- (10) Blockhuys, S.; Wittung-Stafshede, P. Copper Chaperone Atox1 Plays Role in Breast Cancer Cell Migration. *Biochem. Biophys. Res. Commun.* **2017**, *483* (1), 301–304.
- (11) Weekley, C. M.; He, C. Developing Drugs Targeting Transition Metal Homeostasis. *Curr. Opin. Chem. Biol.* **2017**, *37*, 26–32.

- 1
2
3 (12) Wang, J.; Luo, C.; Shan, C.; You, Q.; Lu, J.; Elf, S.; Zhou, Y.; Wen, Y.; Vinkenborg, J. L.;
4 Fan, J.; Kang, H.; Lin, R.; Han, D.; Xie, Y.; Karpus, J.; Chen, S.; Ouyang, S.; Luan, C.;
5 Zhang, N.; Ding, H.; Merckx, M.; Liu, H.; Chen, J.; Jiang, H.; He, C. Inhibition of Human
6 Copper Trafficking by a Small Molecule Significantly Attenuates Cancer Cell Proliferation.
7 *Nat. Chem.* **2015**, *7* (12), 968–979.
8
9
10
11 (13) Wang And, X.; Guo, Z. The Role of Sulfur in Platinum Anticancer Chemotherapy.
12 *Anticancer. Agents Med. Chem.* **2007**, *7* (1), 19–34.
13
14 (14) Legin, A. A.; Schintlmeister, A.; Jakupec, M. A.; Galanski, M.; Lichtscheidl, I.; Wagner, M.;
15 Keppler, B. K. NanoSIMS Combined with Fluorescence Microscopy as a Tool for
16 Subcellular Imaging of Isotopically Labeled Platinum-Based Anticancer Drugs. *Chem. Sci.*
17 **2014**, *5* (8), 3135–3143.
18
19 (15) Spreckelmeyer, S.; Orvig, C.; Casini, A. Cellular Transport Mechanisms of Cytotoxic
20 Metallo drugs: An Overview beyond Cisplatin. *Molecules* **2014**, *19* (10), 15584–15610.
21
22 (16) Calandrini, V.; Rossetti, G.; Arnesano, F.; Natile, G.; Carloni, P. Computational Metallomics
23 of the Anticancer Drug Cisplatin. *J. Inorg. Biochem.* **2015**, *153*, 231–238.
24
25 (17) Messori, L.; Merlino, A. Cisplatin Binding to Proteins: A Structural Perspective. *Coord.*
26 *Chem. Rev.* **2016**, *315*, 67–89.
27
28 (18) Safaei, R.; Howell, S. B. Copper Transporters Regulate the Cellular Pharmacology and
29 Sensitivity to Pt Drugs. *Crit. Rev. Oncol. Hematol.* **2005**, *53* (1), 13–23.
30
31 (19) Gupta, A.; Lutsenko, S. Human Copper Transporters: Mechanism, Role in Human Diseases
32 and Therapeutic Potential. *Future Med. Chem.* **2009**, *1* (6), 1125–1142.
33
34 (20) Lai, Y.-H.; Kuo, C.; Kuo, M.; Chen, H.; Lai, Y.-H.; Kuo, C.; Kuo, M. T.; Chen, H. H. W.
35 Modulating Chemosensitivity of Tumors to Platinum-Based Antitumor Drugs by
36 Transcriptional Regulation of Copper Homeostasis. *Int. J. Mol. Sci.* **2018**, *19* (5), 1486.
37
38 (21) Cepeda, V.; Fuertes, M.; Castilla, J.; Alonso, C.; Quevedo, C.; Perez, J. Biochemical
39 Mechanisms of Cisplatin Cytotoxicity. *Anticancer. Agents Med. Chem.* **2007**, *7* (1), 3–18.
40
41 (22) Gibson, D. The Mechanism of Action of Platinum Anticancer Agents - What Do We Really
42 Know about It? *Dalt. Trans.* **2009**, No. 48, 10681–10689.
43
44 (23) Sancho-Martínez, S. M.; Prieto-García, L.; Prieto, M.; López-Novoa, J. M.; López-
45 Hernández, F. J. Subcellular Targets of Cisplatin Cytotoxicity: An Integrated View.
46 *Pharmacol. Ther.* **2012**, *136* (1), 35–55.
47
48 (24) Corte-Rodríguez, M.; Espina, M.; Sierra, L. M.; Blanco, E.; Ames, T.; Montes-Bayón, M.;
49 Sanz-Medel, A. Quantitative Evaluation of Cellular Uptake, DNA Incorporation and Adduct
50 Formation in Cisplatin Sensitive and Resistant Cell Lines: Comparison of Different Pt-
51
52
53
54
55
56
57
58
59
60

- 1
2
3 Containing Drugs. *Biochem. Pharmacol.* **2015**, *98* (1), 69–77.
- 4
5 (25) Novohradsky, V.; Zerzankova, L.; Stepankova, J.; Vrana, O.; Raveendran, R.; Gibson, D.;
6 Kasparkova, J.; Brabec, V. New Insights into the Molecular and Epigenetic Effects of
7 Antitumor Pt(IV)-Valproic Acid Conjugates in Human Ovarian Cancer Cells. *Biochem.*
8 *Pharmacol.* **2015**, *95* (3), 133–144.
- 9
10
11 (26) Novohradsky, V.; Zanellato, I.; Marzano, C.; Pracharova, J.; Kasparkova, J.; Gibson, D.;
12 Gandin, V.; Osella, D.; Brabec, V. Epigenetic and Antitumor Effects of Platinum(IV)-
13 Octanoato Conjugates. *Sci. Rep.* **2017**, *7* (1), 3751.
- 14
15 (27) Kasherman, Y.; Sturup, S.; Gibson, D. Is Glutathione the Major Cellular Target of Cisplatin?
16 A Study of the Interactions of Cisplatin with Cancer Cell Extracts. *J. Med. Chem.* **2009**, *52*
17 (14), 4319–4328.
- 18
19 (28) Mezencev, R. Interactions of Cisplatin with Non-DNA Targets and Their Influence on
20 Anticancer Activity and Drug Toxicity: The Complex World of the Platinum Complex. *Curr.*
21 *Cancer Drug Targets* **2015**, *14* (9), 794–816.
- 22
23 (29) Mandic, A.; Hansson, J.; Linder, S.; Shoshan, M. C. Cisplatin Induces Endoplasmic
24 Reticulum Stress and Nucleus-Independent Apoptotic Signaling. *J. Biol. Chem.* **2003**, *278*
25 (11), 9100–9106.
- 26
27 (30) Berndtsson, M.; Hägg, M.; Panaretakis, T.; Havelka, A. M.; Shoshan, M. C.; Linder, S.
28 Acute Apoptosis by Cisplatin Requires Induction of Reactive Oxygen Species but Is Not
29 Associated with Damage to Nuclear DNA. *Int. J. Cancer* **2007**, *120* (1), 175–180.
- 30
31 (31) Yu, F.; Megyesi, J.; Price, P. M. Cytoplasmic Initiation of Cisplatin Cytotoxicity. *AJP Ren.*
32 *Physiol.* **2008**, *295* (1), F44–F52.
- 33
34 (32) Gonzalez, V. M.; Fuertes, M. a; Alonso, C.; Perez, J. M. Is Cisplatin-Induced Cell Death
35 Always Produced by Apoptosis? *Mol. Pharmacol.* **2001**, *59* (4), 657–663.
- 36
37 (33) Galluzzi, L.; Vitale, I.; Michels, J.; Brenner, C.; Szabadkai, G.; Harel-Bellan, A.; Castedo,
38 M.; Kroemer, G. Systems Biology of Cisplatin Resistance: Past, Present and Future. *Cell*
39 *Death Dis.* **2014**, *5* (5), e1257.
- 40
41 (34) Bruno, P. M.; Liu, Y.; Park, G. Y.; Murai, J.; Koch, C. E.; Eisen, T. J.; Pritchard, J. R.;
42 Pommier, Y.; Lippard, S. J.; Hemann, M. T. A Subset of Platinum-Containing
43 Chemotherapeutic Agents Kills Cells by Inducing Ribosome Biogenesis Stress. *Nat. Med.*
44 **2017**, *23* (4), 461–471.
- 45
46 (35) Jamieson, E. R.; Lippard, S. J. Structure, Recognition, and Processing of Cisplatin–DNA
47 Adducts. *Chem. Rev.* **1999**, *99* (9), 2467–2498.
- 48
49 (36) Hall, M. D.; Okabe, M.; Shen, D.-W.; Liang, X.-J.; Gottesman, M. M. The Role of Cellular

- 1
2
3 Accumulation in Determining Sensitivity to Platinum-Based Chemotherapy. *Annu. Rev.*
4 *Pharmacol. Toxicol.* **2008**, *48* (1), 495–535.
- 5
6 (37) Heffeter, P.; Jungwirth, U.; Jakupec, M.; Hartinger, C.; Galanski, M.; Elbling, L.; Micksche,
7 M.; Keppler, B.; Berger, W. Resistance against Novel Anticancer Metal Compounds:
8 Differences and Similarities. *Drug Resist. Updat.* **2008**, *11* (1–2), 1–16.
- 9
10 (38) Safaei, R.; Maktabi, M. H.; Blair, B. G.; Larson, C. A.; Howell, S. B. Effects of the Loss of
11 Atox1 on the Cellular Pharmacology of Cisplatin. *J. Inorg. Biochem.* **2009**, *103* (3), 333–
12 341.
- 13
14 (39) Palm, M. E.; Weise, C. F.; Lundin, C.; Wingsle, G.; Nygren, Y.; Bjorn, E.; Naredi, P.; Wolf-
15 Watz, M.; Wittung-Stafshede, P. Cisplatin Binds Human Copper Chaperone Atox1 and
16 Promotes Unfolding in Vitro. *Proc. Natl. Acad. Sci.* **2011**, *108* (17), 6951–6956.
- 17
18 (40) Samimi, G.; Katano, K.; Holzer, A. K.; Safaei, R.; Howell, S. B. Modulation of the Cellular
19 Pharmacology of Cisplatin and Its Analogs by the Copper Exporters ATP7A and ATP7B.
20 *Mol. Pharmacol.* **2004**, *66* (1), 25–32.
- 21
22 (41) Ciarimboli, G. Membrane Transporters as Mediators of Cisplatin Side-Effects. *Anticancer*
23 *Res.* **2014**, *34* (1), 547–550.
- 24
25 (42) Samimi, G.; Safaei, R.; Katano, K.; Holzer, A. K.; Rochdi, M.; Tomioka, M.; Goodman, M.;
26 Howell, S. B. Increased Expression of the Copper Efflux Transporter ATP7A Mediates
27 Resistance to Cisplatin, Carboplatin, and Oxaliplatin in Ovarian Cancer Cells. *Clin. Cancer*
28 *Res.* **2004**, *10* (14), 4661–4669.
- 29
30 (43) Kalayda, G. V.; Wagner, C. H.; Buß, I.; Reedijk, J.; Jaehde, U. Altered Localisation of the
31 Copper Efflux Transporters ATP7A and ATP7B Associated with Cisplatin Resistance in
32 Human Ovarian Carcinoma Cells. *BMC Cancer* **2008**, *8*, 175.
- 33
34 (44) Tadini-Buoninsegni, F.; Bartolommei, G.; Rosa Moncelli, M.; Inesi, G.; Galliani, A.; Sinisi,
35 M.; Losacco, M.; Natile, G.; Arnesano, F. Translocation of Platinum Anticancer Drugs by
36 Human Copper ATPases ATP7A and ATP7B. *Angew. Chemie - Int. Ed.* **2014**, *53* (5), 1297–
37 1301.
- 38
39 (45) Galliani, A.; Losacco, M.; Lasorsa, A.; Natile, G.; Arnesano, F. Cisplatin Handover between
40 Copper Transporters: The Effect of Reducing Agents. *J. Biol. Inorg. Chem.* **2014**, *19* (4–5),
41 705–714.
- 42
43 (46) Xi, Z.; Guo, W.; Tian, C.; Wang, F.; Liu, Y. Copper Binding Promotes the Interaction of
44 Cisplatin with Human Copper Chaperone Atox1. *Chem. Commun.* **2013**, *49* (95), 11197–
45 11199.
- 46
47 (47) Fang, T.; Tian, Y.; Yuan, S.; Sheng, Y.; Arnesano, F.; Natile, G.; Liu, Y. Differential
48
49
50
51
52
53
54
55
56
57
58
59
60

- 1
2
3 Reactivity of Metal Binding Domains of Copper ATPases towards Cisplatin and
4 Colocalization of Copper and Platinum. *Chem. - A Eur. J.* **2018**, *24* (36), 8999–9003.
- 5
6 (48) Banci, L.; Bertini, I.; Calderone, V.; Della-Malva, N.; Felli, I. C.; Neri, S.; Pavelkova, A.;
7 Rosato, A. Copper(I)-Mediated Protein–protein Interactions Result from Suboptimal
8 Interaction Surfaces. *Biochem. J.* **2009**, *422* (1), 37–42.
- 9
10 (49) Banci, L.; Bertini, I.; Cantini, F.; Felli, I. C.; Gonnelli, L.; Hadjiliadis, N.; Pierattelli, R.;
11 Rosato, A.; Voulgaris, P. The Atx1-Ccc2 Complex Is a Metal-Mediated Protein-Protein
12 Interaction. *Nat. Chem. Biol.* **2006**, *2* (7), 367–368.
- 13
14 (50) Xiao, Z.; Brose, J.; Schimo, S.; Ackland, S. M.; La Fontaine, S.; Wedd, A. G. Unification of
15 the Copper(I) Binding Affinities of the Metallo-Chaperones Atx1, Atox1, and Related
16 Proteins: Detection Probes and Affinity Standards. *J. Biol. Chem.* **2011**, *286* (13), 11047–
17 11055.
- 18
19 (51) Badarau, A.; Baslé, A.; Firbank, S. J.; Dennison, C. Crosstalk between Cu(I) and Zn(II)
20 Homeostasis via Atx1 and Cognate Domains. *Chem. Commun.* **2013**, *49* (73), 8000–8002.
- 21
22 (52) Corazza, A.; Harvey, I.; Sadler, P. J. ¹H,¹³C-NMR and X-Ray Absorption Studies of
23 Copper(I) Glutathione Complexes. *Eur. J. Biochem.* **1996**, *236*, 697–705.
- 24
25 (53) Huffman, D. L.; O’Halloran, T. V. Energetics of Copper Trafficking between the Atx1
26 Metallochaperone and the Intracellular Copper Transporter, Ccc2. *J. Biol. Chem.* **2000**, *275*
27 (25), 18611–18614.
- 28
29 (54) Pufahl, R. A.; Singer, C. P.; Peariso, K. L.; Lin, S. J.; Schmidt, P. J.; Fahrni, C. J.; Cizewski
30 Culotta, V.; Penner-Hahn, J. E.; O’Halloran, T. V. Metal Ion Chaperone Function of the
31 Soluble Cu(I) Receptor Atx1. *Science* **1997**, *278* (5339), 853–856.
- 32
33 (55) Berners-Price, S. J.; Ronconi, L.; Sadler, P. J. Insights into the Mechanism of Action of
34 Platinum Anticancer Drugs from Multinuclear NMR Spectroscopy. *Prog. Nucl. Magn.*
35 *Reson. Spectrosc.* **2006**, *49* (1), 65–98.
- 36
37 (56) Arnesano, F.; Banci, L.; Bertini, I.; Felli, I. C.; Losacco, M.; Natile, G. Probing the
38 Interaction of Cisplatin with the Human Copper Chaperone Atox1 by Solution and In-Cell
39 NMR Spectroscopy. *J. Am. Chem. Soc.* **2011**, *133* (45), 18361–18369.
- 40
41 (57) Arnesano, F.; Natile, G. “Platinum on the Road”: Interactions of Antitumoral Cisplatin with
42 Proteins. *Pure Appl. Chem.* **2008**, *80* (12), 2715–2725.
- 43
44 (58) Belviso, B. D.; Galliani, A.; Lasorsa, A.; Mirabelli, V.; Caliandro, R.; Arnesano, F.; Natile,
45 G. Oxaliplatin Binding to Human Copper Chaperone Atox1 and Protein Dimerization. *Inorg.*
46 *Chem.* **2016**, *55* (13), 6563–6573.
- 47
48 (59) Cunningham, R. M.; DeRose, V. J. Platinum Binds Proteins in the Endoplasmic Reticulum of

- 1
2
3 S. *Cerevisiae* and Induces Endoplasmic Reticulum Stress. *ACS Chem. Biol.* **2017**, *12* (11),
4 2737–2745.
5
6 (60) Öhrvik, H.; Wittung-Stafshede, P.; Öhrvik, H.; Wittung-Stafshede, P. Identification of New
7 Potential Interaction Partners for Human Cytoplasmic Copper Chaperone Atox1: Roles in
8 Gene Regulation? *Int. J. Mol. Sci.* **2015**, *16* (8), 16728–16739.
9
10 (61) Gorrini, C.; Harris, I. S.; Mak, T. W. Modulation of Oxidative Stress as an Anticancer
11 Strategy. *Nat. Rev. Drug Discov.* **2013**, *12* (12), 931–947.
12
13 (62) Mercer, J. F. B.; Barnes, N.; Stevenson, J.; Strausak, D.; Llanos, R. M. Copper-Induced
14 Trafficking of the Cu-ATPases: A Key Mechanism for Copper Homeostasis. *BioMetals*
15 **2003**, *16* (1), 175–184.
16
17 (63) Amoresano, A.; Chang, C. J.; Chan, J.; Pucci, P.; Piccolo, P.; Pane, F.; Parenti, G.; Concilli,
18 M.; Polishchuk, R. S.; Paladino, S.; Polishchuk, E. V.; Chesi, G.; Baldantoni, D.; van
19 IJzendoorn, S. C. D.; Settembre, C.; Pastore, N.; Tarallo, A.; Brunetti-Pierri, N.; Iacobacci,
20 S.; Ballabio, A. Wilson Disease Protein ATP7B Utilizes Lysosomal Exocytosis to Maintain
21 Copper Homeostasis. *Dev. Cell* **2014**, *29* (6), 686–700.
22
23 (64) LeShane, E. S.; Shinde, U.; Walker, J. M.; Barry, A. N.; Blackburn, N. J.; Ralle, M.;
24 Lutsenko, S. Interactions between Copper-Binding Sites Determine the Redox Status and
25 Conformation of the Regulatory N-Terminal Domain of ATP7B. *J. Biol. Chem.* **2010**, *285*,
26 6327–6336.
27
28 (65) Lim, C. M.; Cater, M. A.; Mercer, J. F. B.; La Fontaine, S. Copper-Dependent Interaction of
29 Dynactin Subunit P62 with the N Terminus of ATP7B but Not ATP7A. *J. Biol. Chem.* **2006**,
30 *281* (20), 14006–14014.
31
32 (66) Arnesano, F.; Nardella, M. I.; Natile, G. Platinum Drugs, Copper Transporters and Copper
33 Chelators. *Coord. Chem. Rev.* **2018**, *374*, 254–260.
34
35 (67) Wouters, E. F. M.; Savelkoul, P. H. M.; Benedikter, B. J.; Stassen, F. R. M.; Weseler, A. R.;
36 Rohde, G. G. U. Redox-Dependent Thiol Modifications: Implications for the Release of
37 Extracellular Vesicles. *Cell. Mol. Life Sci.* **2018**, *75* (13), 2321–2337.
38
39 (68) Chisholm, C. L.; Wang, H.; Hang-Heng Wong, A.; Vazquez-Ortiz, G.; Chen, W.; Xu, X.;
40 Deng, C.-X. Ammonium Tetrathiomolybdate Treatment Targets the Copper Transporter
41 ATP7A and Enhances Sensitivity of Breast Cancer to Cisplatin. *Oncotarget* **2016**, *7* (51),
42 84439–84452.
43
44 (69) Tian, Y.; Fang, T.; Yuan, S.; Zheng, Y.; Arnesano, F.; Natile, G.; Liu, Y. Tetrathiomolybdate
45 Inhibits the Reaction of Cisplatin with Human Copper Chaperone Atox1. *Metallomics* **2018**,
46 *10* (5), 745–750.
47
48
49
50
51
52
53
54
55
56
57
58
59
60

- 1
2
3 (70) Alvarez, H. M.; Xue, Y.; Robinson, C. D.; Canalizo-Hernández, M. A.; Marvin, R. G.; Kelly,
4 R. A.; Mondragón, A.; Penner-Hahn, J. E.; O'Halloran, T. V. Tetrathiomolybdate Inhibits
5 Copper Trafficking Proteins Through Metal Cluster Formation. *Science* **2010**, *327* (5963),
6 331–334.
7
8
9
10 (71) Akerfeldt, M. C.; Tran, C. M.-N.; Shen, C.; Hambley, T. W.; New, E. J. Interactions of
11 Cisplatin and the Copper Transporter CTR1 in Human Colon Cancer Cells. *J. Biol. Inorg.*
12 *Chem.* **2017**, *22* (5), 765–774.
13
14
15 (72) Spreckelmeyer, S.; van der Zee, M.; Bertrand, B.; Bodio, E.; Stürup, S.; Casini, A. Relevance
16 of Copper and Organic Cation Transporters in the Activity and Transport Mechanisms of an
17 Anticancer Cyclometallated Gold(III) Compound in Comparison to Cisplatin. *Front. Chem.*
18 **2018**, *6*, 377.
19
20
21
22
23
24
25
26
27
28
29
30
31
32
33
34
35
36
37
38
39
40
41
42
43
44
45
46
47
48
49
50
51
52
53
54
55
56
57
58
59
60

Table of Contents (TOC) graphic